Supplemental Information

Bridging Cyanides from Cyanoiron Metalloligands to Redox-active Dinitrosyl Iron Units

Pokhraj Ghosh[#,‡], Manuel Quiroz[#,‡], Randara Pulukkody[#], Nattamai Bhuvanesh,[#] and Marcetta Y. Darensbourg[#,*]

[#]*Department of Chemistry, Texas A & M University, College Station, Texas 77843, United States*
[‡]*Equally contributing authors*

Reactivity Studies

For every Me_3P reactivity study, 0.1 mL of Me_3P was added to 10 mL of THF to generate a 0.097 M stock solution of Me_3P.

Reaction of Fe-1 with Me_3P. Approximately144 μL of a 0.097 M solution (1 equivalent, 0.014 mmol)of Me_3P was added to a THF solution containing 15 mg (0.014 mmol) of [(dppe)(η^5-C_5H_5)Fe-CN-$Fe(NO)_2$(IMes)][BF_4](Fe-1) 25 mins. Reaction completion and formation of $(Me_3P)_2Fe(NO)_2$was monitored by IR spectroscopy after every equivalence of Me_3P was added (7 total equivalence).

Reaction of Fe*-1 with Me_3P. Approximately 137 μL of a 0.097 M solution (1 equivalent, 0.013 mmol) of Me_3P was added to a THF solution containing 15 mg (0.013 mmol) of [(dppe)(η^5-C_5Me_5)Fe-CN-$Fe(NO)_2$(IMes)][BF_4](Fe*-1) every 25 mins. Reaction completion and formation of $(Me_3P)_2Fe(NO)_2$was monitored by IR spectroscopy after every equivalence of Me_3P was added (7 total equivalence).

Reaction of Fe*-2 with Me_3P.In a 50 mL Schlenk flask approximately 0.134 g (0.1 mmol) of freshly prepared [((dppe)(η^5-C_5Me_5)Fe-CN)$_2$-$Fe(NO)_2$]in THF was reacted with excess Me_3P (0.20 mL, 2.0 mmol) by stirring at –5 °C. Reaction competition and formation of $(Me_3P)_2Fe(NO)_2$ was monitored by IR spectroscopy.

Reaction of Fe-1 with Na^+SPh^-. Approximately 3.7 mg (0.028 mmol) of sodium phenolate in THF was added to a flask containing 15 mg (0.014 mmol) of [(dppe)(η^5-C_5H_5)Fe-CN-$Fe(NO)_2$(IMes)][BF_4](Fe-1). Reaction was done in the time of mixing giving an orange-red colored solution and the formation of $IMesFe(NO)_2(SPh)$ was confirmed through IR spectroscopy.

Reaction of Fe*-1 with Na^+SPh^-. Approximately 3.5 mg (0.026 mmol) of sodium phenolate in THF was added to a flask containing 15 mg (0.013 mmol) of [(dppe)(η^5-C_5Me_5)Fe-CN-$Fe(NO)_2$(IMes)][BF_4](Fe-1). Reaction was done in the time of mixing giving an orange-red colored solution and the formation of $IMesFe(NO)_2(SPh)$ was confirmed through IR spectroscopy.

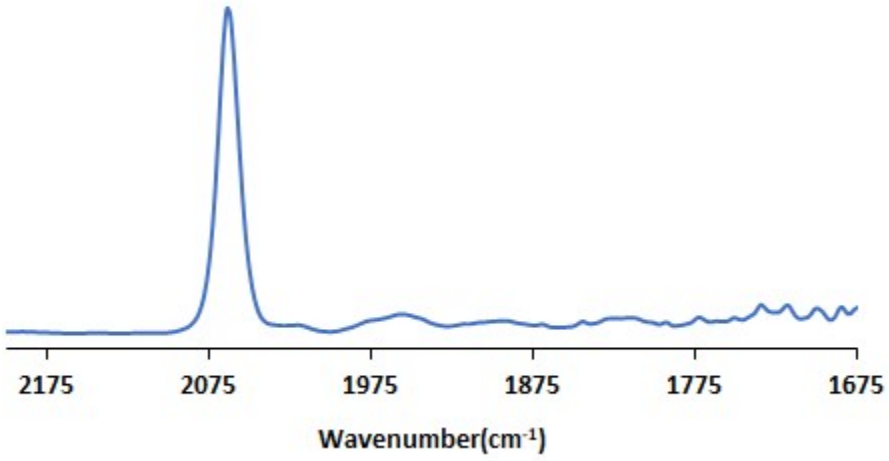

Figure S1. Infrared spectrum of (dppe)(η^5-C_5H_5)Fe(CN) (**Fe'-CN**) in CH_2Cl_2.

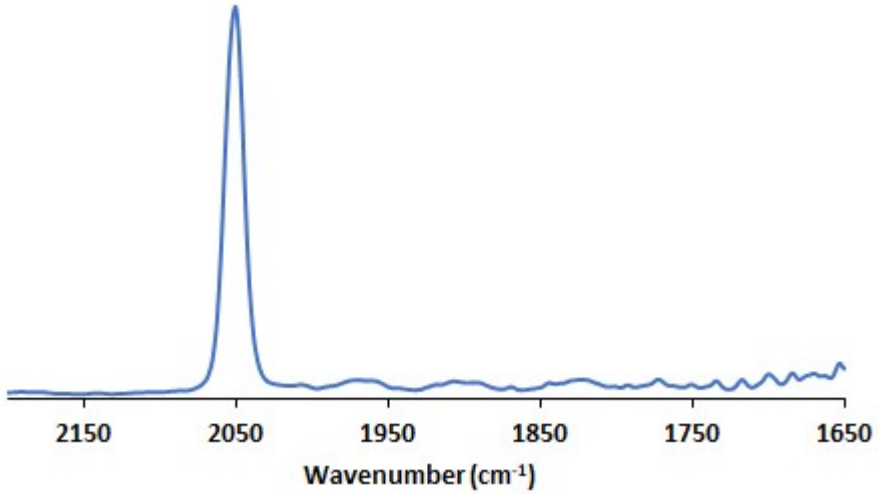

Figure S2. Infrared spectrum of (dppe)(η^5-C_5Me_5)Fe(CN) (**Fe*-CN**) in CH_2Cl_2.

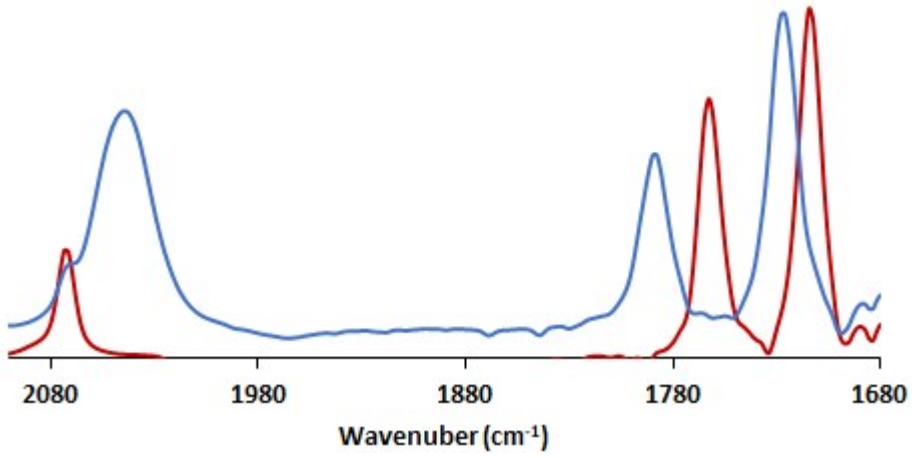

Figure S3. Infrared spectrum of sIMesFe(NO)$_2$(SPh) (in red) after reacting [(dppe)(η^5-C_5H_5)Fe-CN-Fe(NO)$_2$(IMes)][BF_4] (**Fe-1**) (in blue) with sodium phenolate in THF.

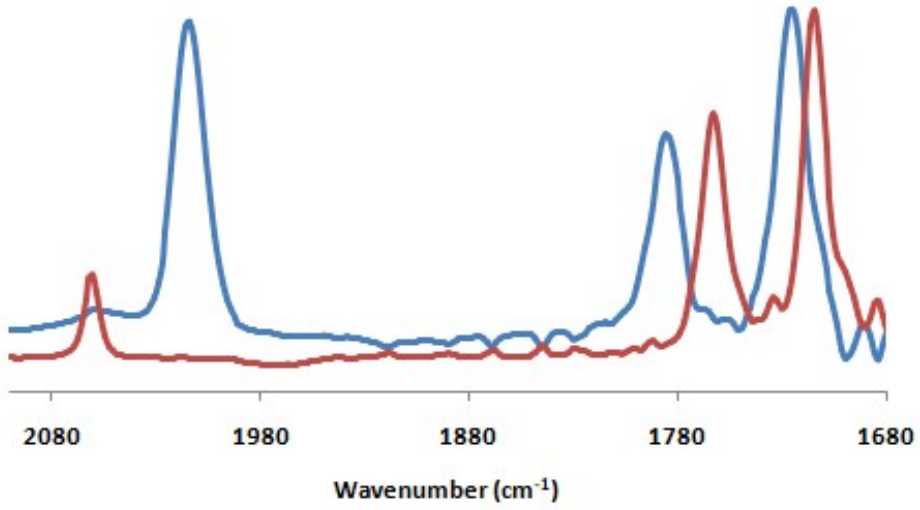

Figure S4. Infrared spectrum of sIMesFe(NO)$_2$(SPh) (in red) after reacting [(dppe)(η^5-C_5Me_5)Fe-CN-Fe(NO)$_2$(IMes)][BF_4] (**Fe*-1**) (in blue) with sodium phenolate in THF.

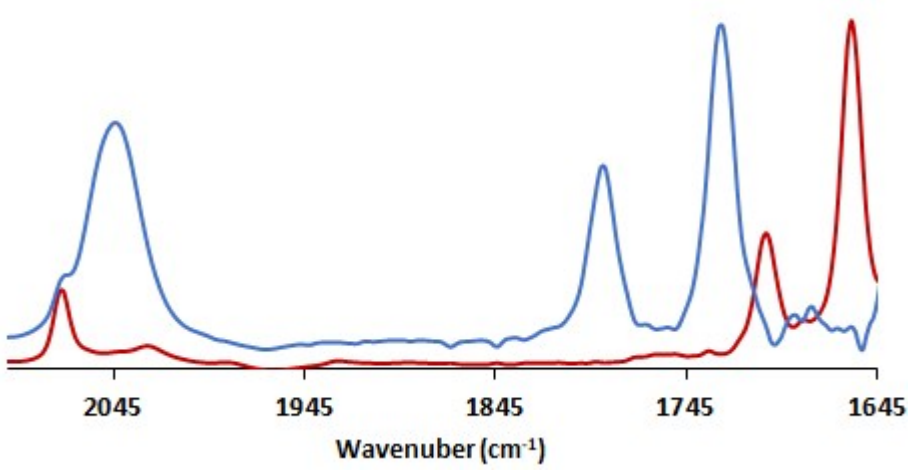

Figure S5. Infrared spectrum of $(Me_3P)_2Fe(NO)_2$ (in red) after reacting $[(dppe)(\eta^5\text{-}C_5H_5)Fe\text{-}CN\text{-}Fe(NO)_2(IMes)][BF_4]$ (**Fe-1**) (in blue) with Me_3P in THF.

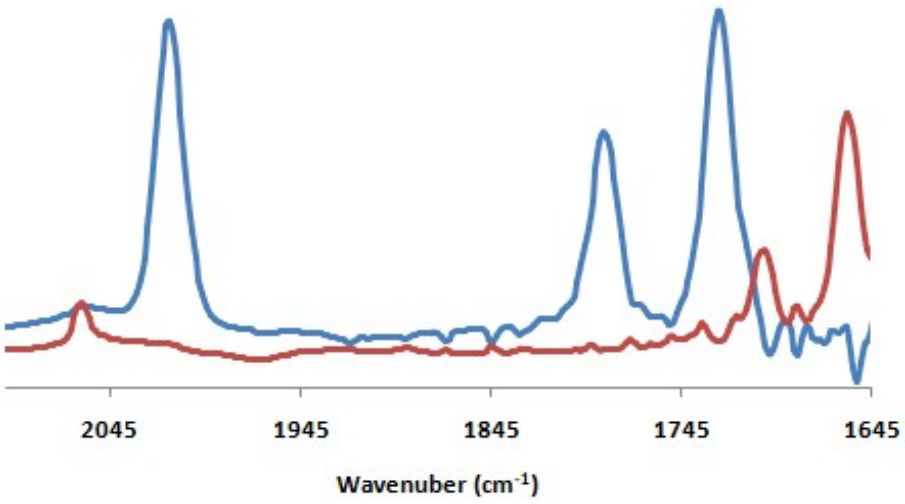

Figure S6. Infrared spectrum of $(Me_3P)Fe(NO)_2$ (in red) after reacting $[(dppe)(\eta^5\text{-}C_5Me_5)Fe\text{-}CN\text{-}Fe(NO)_2(IMes)][BF_4]$ (**Fe*-1**) (in blue) with Me_3P in THF.

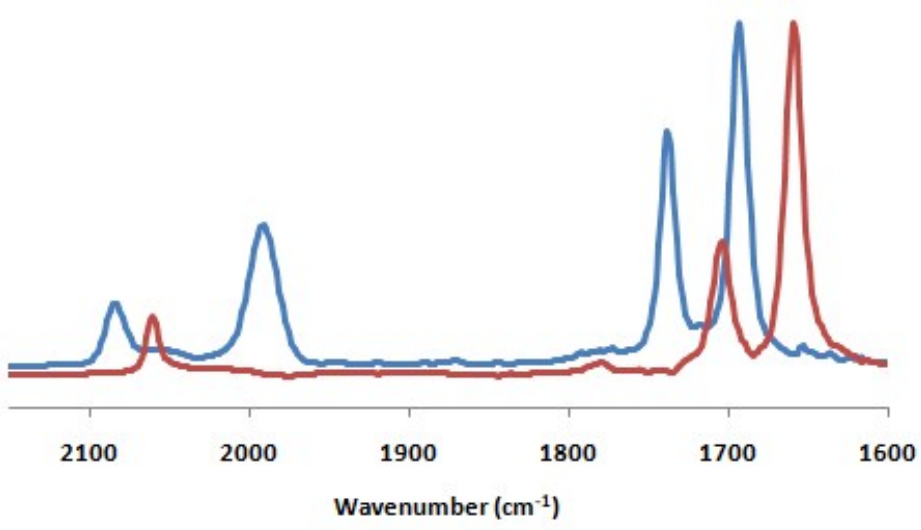

Figure S7. Infrared spectrum of $(Me_3P)Fe(NO)_2$ (in red) after reacting $[(dppe)(\eta^5\text{-}C_5Me_5)Fe\text{-}CN)_2\text{-}Fe(NO)_2]$ (**Fe*-2**) (in blue) with Me_3P in THF at - 5°C.

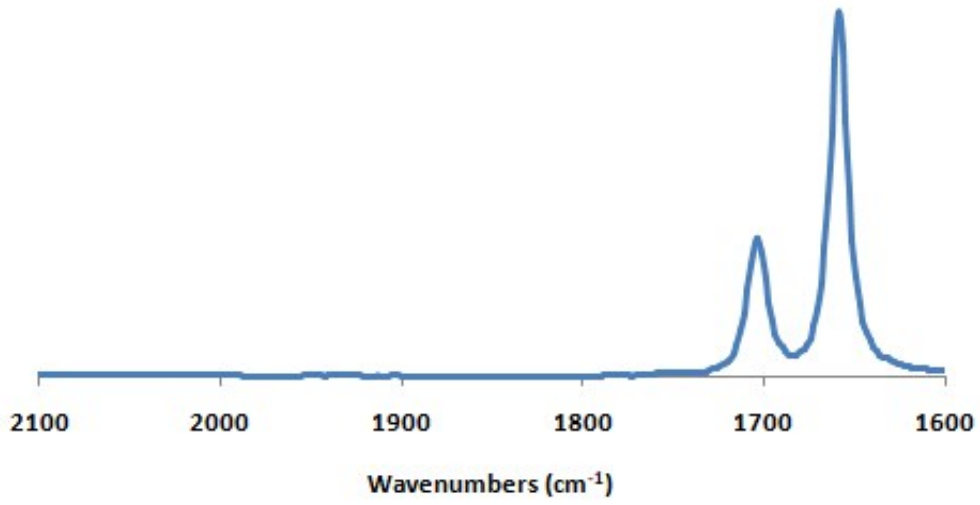

Figure S8. Infrared spectrum of $(Me_3P)_2Fe(NO)_2$ in THF.

Electrochemistry

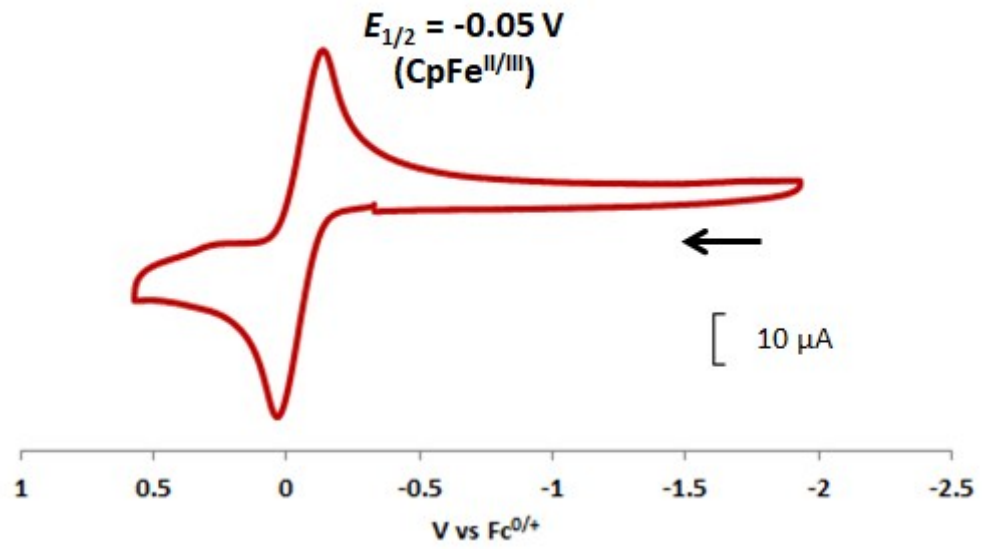

Figure S9. Cyclic voltammogram of (dppe)(η^5-C_5H_5)Fe(CN) (**Fe'-CN**) in CH_2Cl_2 referenced to $Fc^{0/+}$.

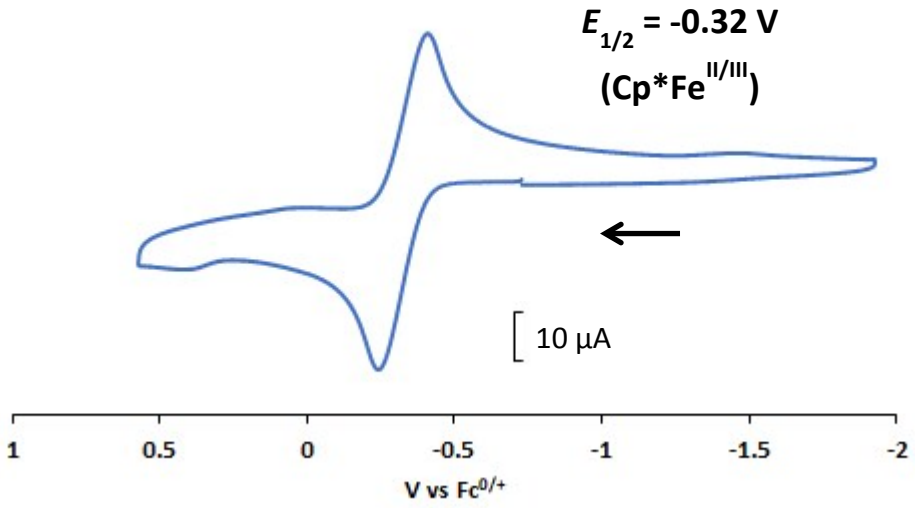

Figure S10. Cyclic voltammogram of (dppe)(η^5-C_5Me_5)Fe(CN) (**Fe*-CN**) in CH_2Cl_2 referenced to $Fc^{0/+}$.

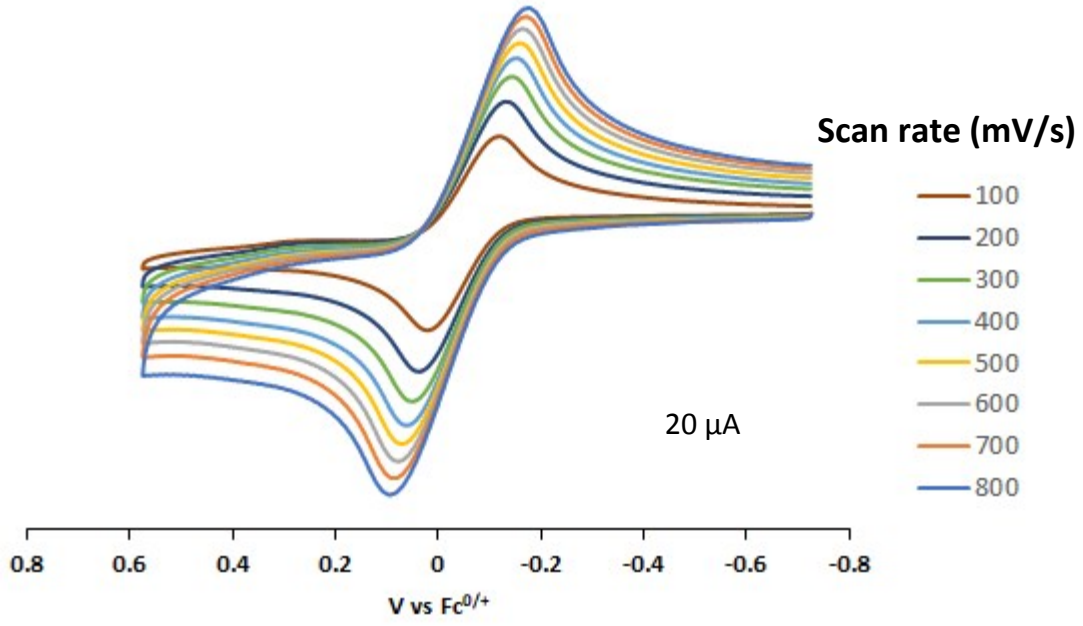

Figure S11. Cyclic voltammogram of (dppe)(η^5-C_5H_5)Fe(CN) (**Fe'-CN**) recorded at different scan rates in DCM referenced to $Fc^{0/+}$.

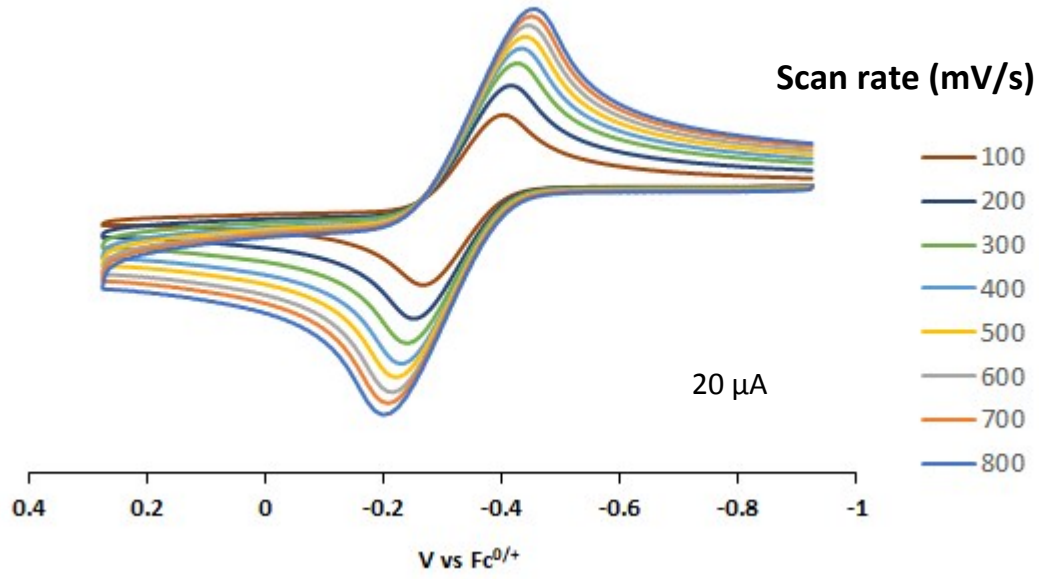

Figure S12. Cyclic voltammogram of (dppe)(η^5-C_5Me_5)Fe(CN) (**Fe*-CN**) recorded at different scan rates in DCM referenced to $Fc^{0/+}$.

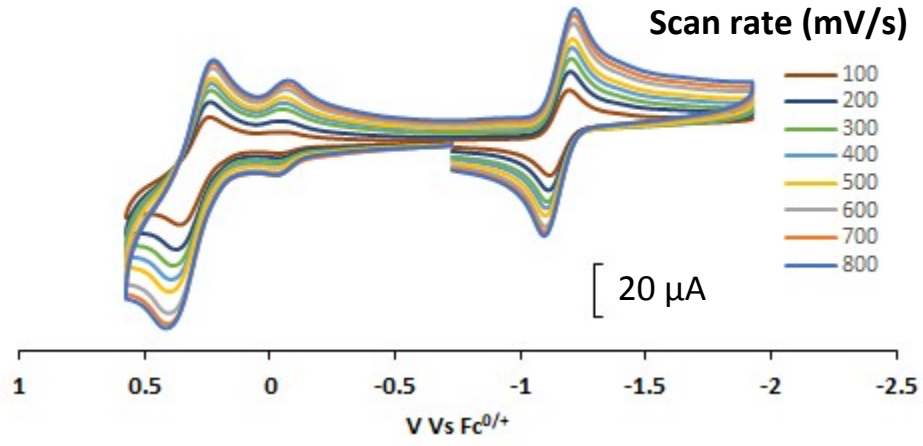

Figure S13. Cyclic voltammogram of [(dppe)(η^5-C_5H_5)Fe-CN-Fe$(NO)_2$(IMes)][BF_4] (**Fe-1**) recorded at different scan rates in DCM referenced to $Fc^{0/+}$.

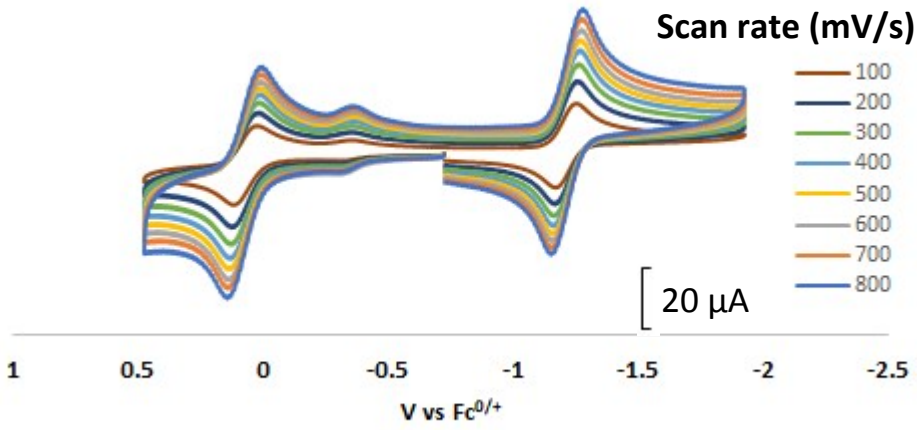

Figure S14. Cyclic voltammogram of [(dppe)(η^5-C_5Me_5)Fe-CN-Fe$(NO)_2$(IMes)][BF_4] (**Fe*-1**) recorded at different scan rates in DCM referenced to $Fc^{0/+}$.

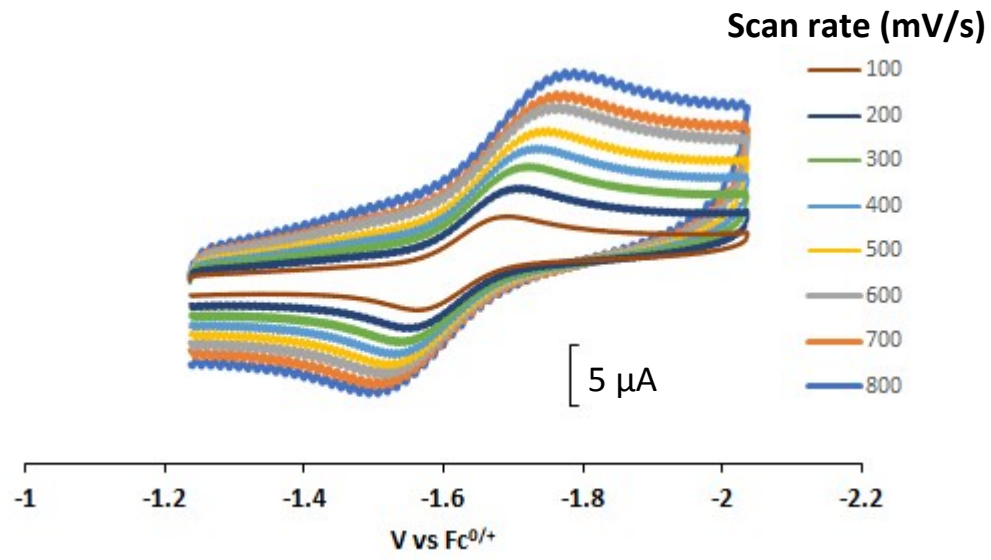

Figure S15. The reduction event, $\{Fe(NO)_2\}^{9/10}$, of $[((dppe)(\eta^5\text{-}C_5Me_5)Fe\text{-}CN)_2\text{-}Fe(NO)_2]$ (**Fe*-2**) recorded at different scan rates in THF referenced to $Fc^{0/+}$.

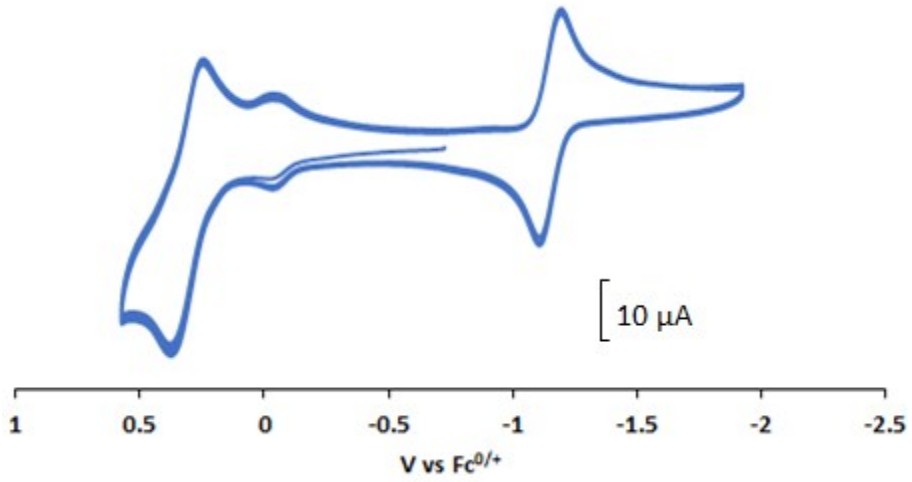

Figure S16. Cyclic voltammogram with repeated scans of $[(dppe)(\eta^5\text{-}C_5H_5)Fe\text{-}CN\text{-}Fe(NO)_2(IMes)][BF_4]$ (**Fe-1**) in DCM referenced to $Fc^{0/+}$.

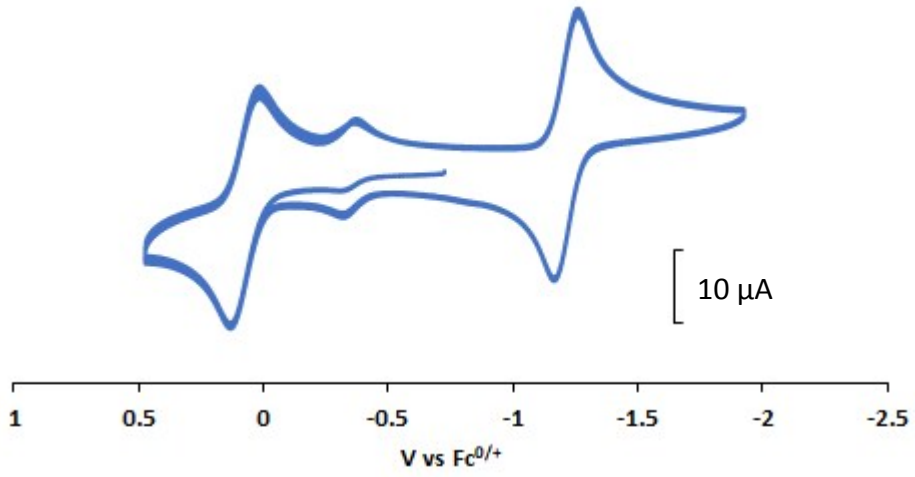

Figure S17. Cyclic voltammogram with repeated scans of [(dppe)(η^5-C_5Me_5)Fe-CN-Fe(NO)$_2$(IMes)][BF_4] (**Fe*-1**) in DCM referenced to $Fc^{0/+}$.

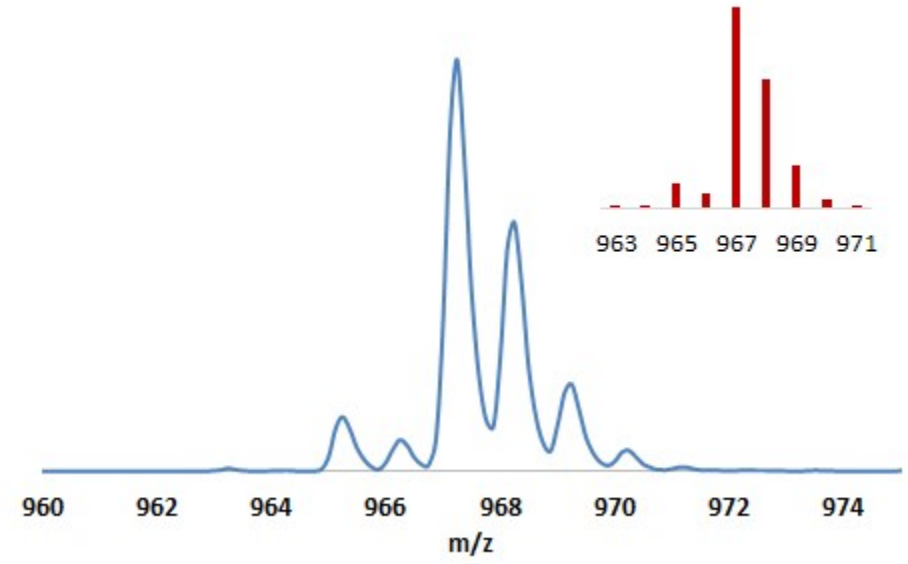

Figure S18. Positive-ion ESI mass spectrum of[(dppe)(η^5-C_5H_5)Fe-CN-Fe(NO)$_2$(IMes)][BF_4] (**Fe-1**) in CH_3CN; inset: Calculated isotopic distribution for complex [(dppe)(η^5-C_5H_5)Fe-CN-Fe(NO)$_2$(IMes)][BF_4] (**Fe-1**).

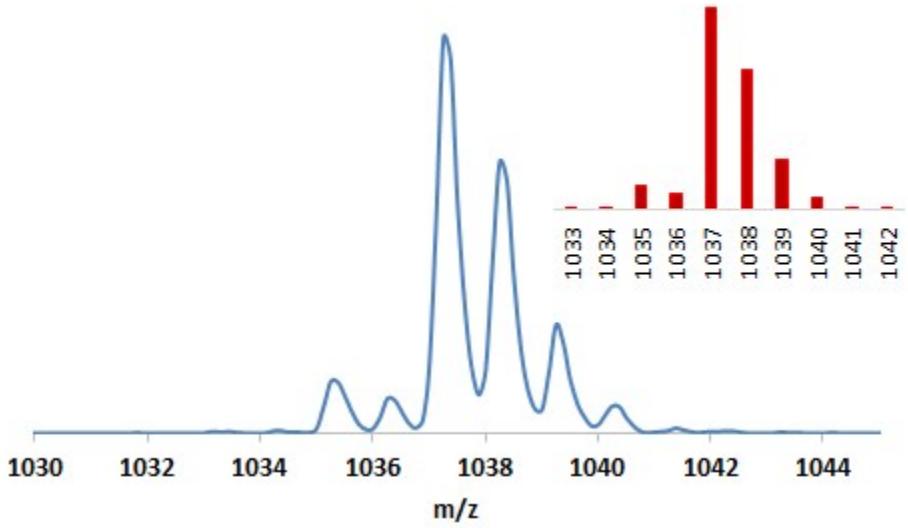

Figure S19. Positive-ion ESI mass spectrum of[(dppe)(η^5-C_5Me_5)Fe-CN-Fe$(NO)_2$(IMes)][BF_4] (**Fe*-1**) in CH_3CN; inset: Calculated isotopic distribution for complex [(dppe)(η^5-C_5Me_5)Fe-CN-Fe$(NO)_2$(IMes)][BF_4] (**Fe*-1**).

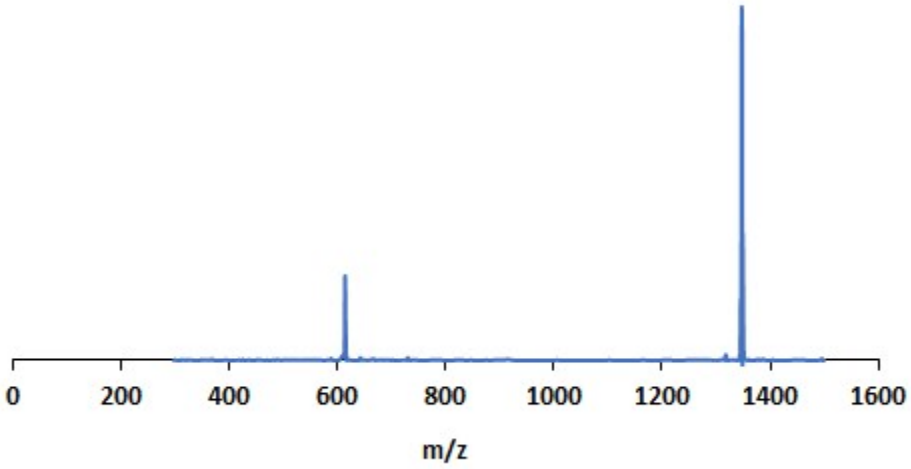

Figure S20. Positive-ion ESI mass spectrum of [((dppe)(η^5-C_5Me_5)Fe-$CN)_2$-Fe$(NO)_2$] (**Fe*-2**) in CH_3CN/THF (1:1 v/v).

Figure S21. Molecular structure of **Fe-1.**

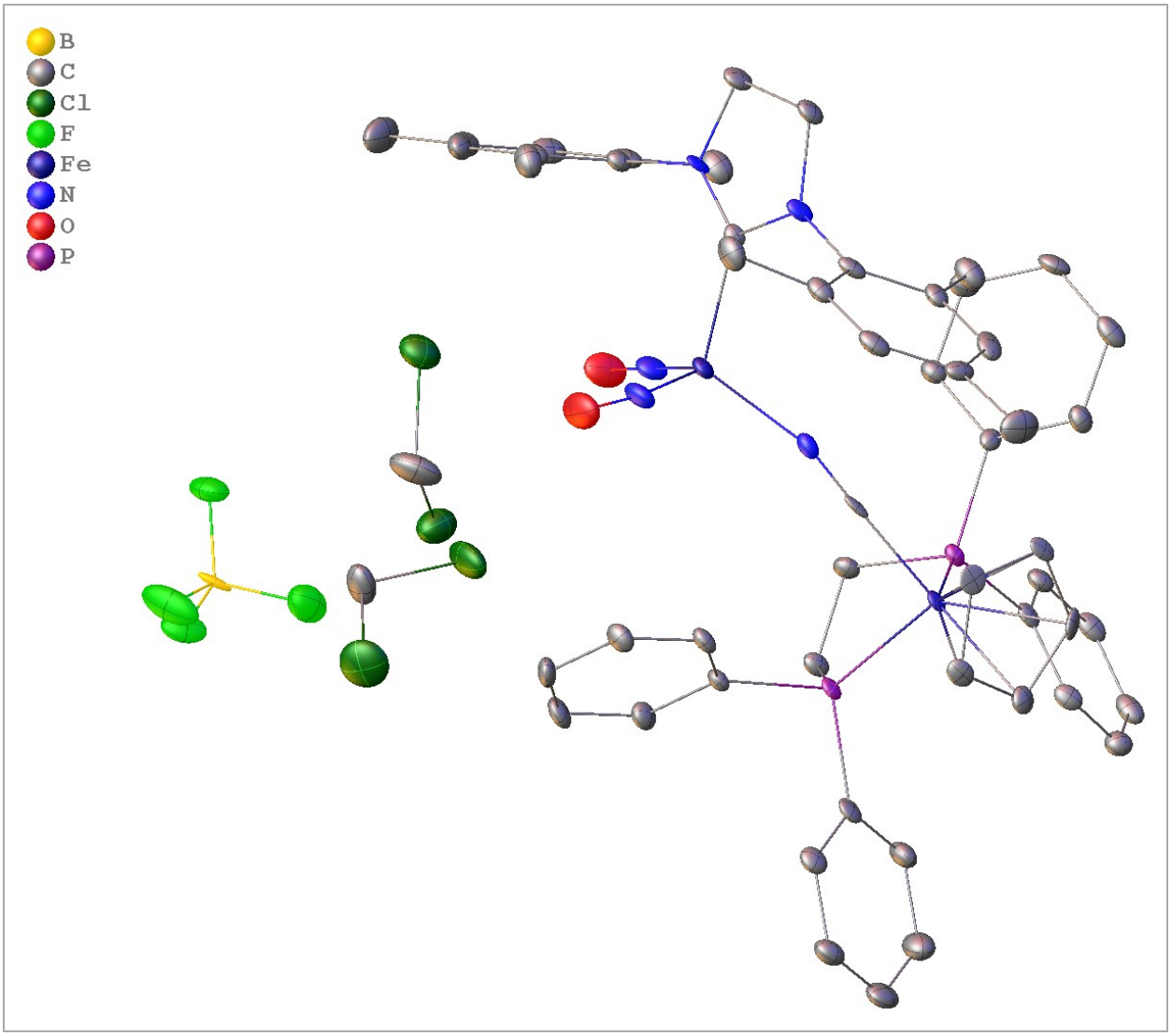

Table T1. Crystal data and structure refinement for **Fe-1.**

Identification code	DPPEFeCN_0m
Empirical formula	$C_{55}H_{59}BCl_4F_4Fe_2N_5O_2P_2$
Formula weight	1224.32
Temperature/K	110.0

Crystal system	triclinic
Space group	P-1
a/Å	13.643(7)
b/Å	14.261(8)
c/Å	14.533(7)
α/°	91.49(3)
β/°	98.57(2)
γ/°	91.66(3)
Volume/Å^3	2794(3)
Z	2
ρ_{calc}g/cm^3	1.456
μ/mm^{-1}	6.960
F(000)	1262.0
Crystal size/mm^3	0.1 × 0.1 × 0.1
Radiation	CuKα (λ = 1.54184)
2Θ range for data collection/°	6.154 to 145.282
Index ranges	-16 ≤ h ≤ 16, -17 ≤ k ≤ 17, -17 ≤ l ≤ 17
Reflections collected	73161
Independent reflections	10802 [R_{int} = 0.0561, R_{sigma} = 0.0330]
Data/restraints/parameters	10802/0/682
Goodness-of-fit on F^2	1.070
Final R indexes [I>=2σ (I)]	R_1 = 0.0756, wR_2 = 0.1766
Final R indexes [all data]	R_1 = 0.0813, wR_2 = 0.1826
Largest diff. peak/hole / e Å^{-3}	1.48/-1.76

Figure S22. Molecular structure of **Fe*-1.**

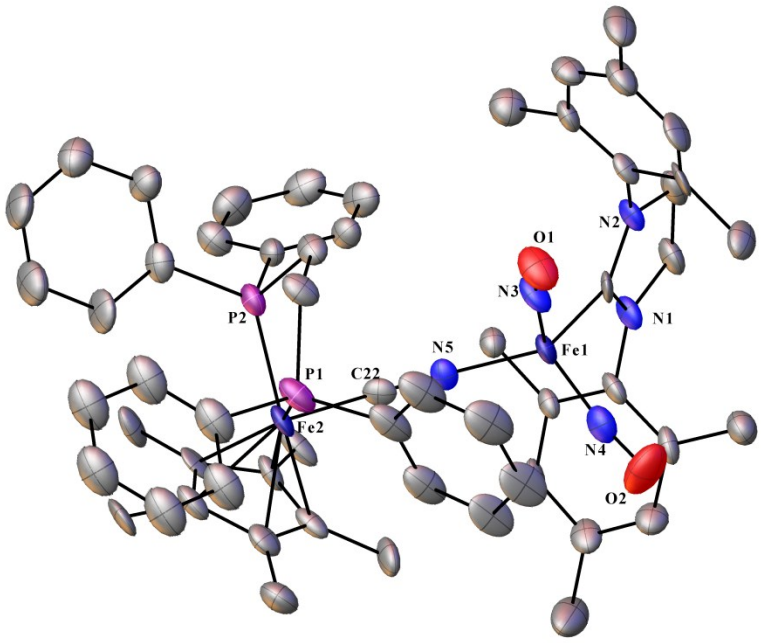

Table T2. Crystal data and structure refinement for Fe*-1.

Identification code	fe5mecntnic_sq	
Empirical formula	C62 H73 B F4 Fe2 N5 O3 P2	
Formula weight	1196.70	
Temperature	100.0 K	
Wavelength	1.54178 Å	
Crystal system	Monoclinic	
Space group	P 1 21/c 1	
Unit cell dimensions	a = 21.1283(8) Å	□= 90°.
	b = 15.3003(5) Å	□= 104.996(2)°.
	c = 23.5487(8) Å	□ = 90°.
Volume	7353.3(4) $Å^3$	
Z	4	
Density (calculated)	1.081 Mg/m^3	
Absorption coefficient	3.981 mm^{-1}	
F(000)	2508	

Crystal size	0.398 x 0.056 x 0.026 mm^3
Theta range for data collection	3.481 to 49.999°.
Index ranges	-20<=h<=20, -14<=k<=15, -23<=l<=23
Reflections collected	126475
Independent reflections	7546 [R(int) = 0.1564]
Completeness to theta = 49.999°	100.0 %
Absorption correction	Semi-empirical from equivalents
Max. and min. transmission	0.7320 and 0.5006
Refinement method	Full-matrix least-squares on F^2
Data / restraints / parameters	7546 / 572 / 785
Goodness-of-fit on F^2	1.138
Final R indices [I>2sigma(I)]	R1 = 0.0908, wR2 = 0.1833
R indices (all data)	R1 = 0.1087, wR2 = 0.1917
Extinction coefficient	n/a
Largest diff. peak and hole	0.761 and -0.425 $e.Å^{-3}$

Figure S23. Molecular structure of **Fe*-CN.**

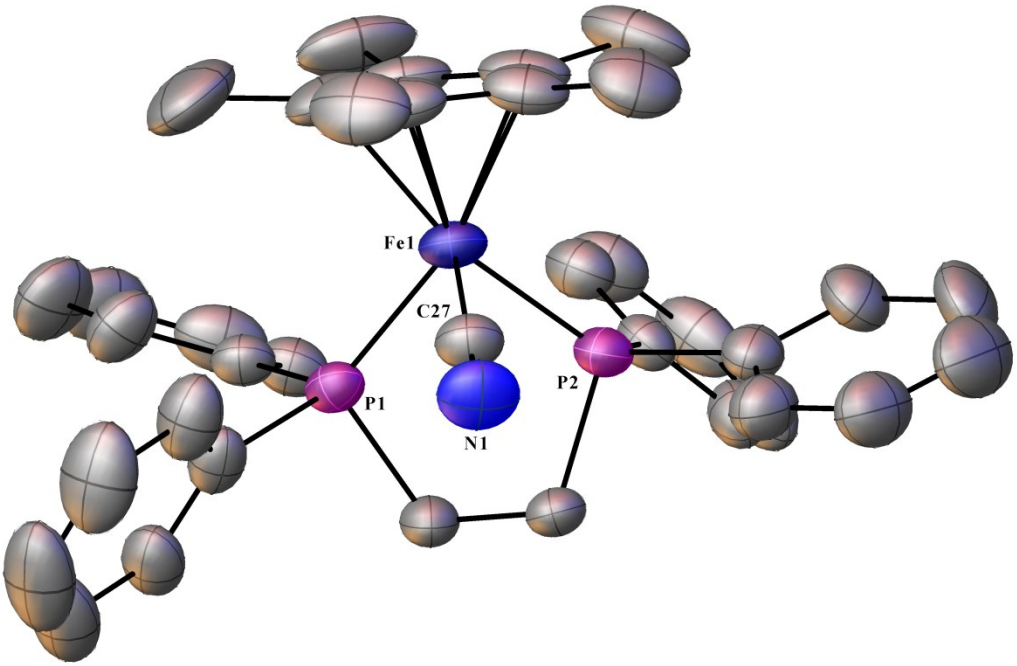

Table T3. Crystal data and structure refinement for **Fe*-CN.**

Identification code	cpmefecn	
Empirical formula	C37 H39 Fe N P2	
Formula weight	615.48	
Temperature	293.0 K	
Wavelength	0.71073 Å	
Crystal system	Monoclinic	
Space group	P 1 21/n 1	
Unit cell dimensions	a = 12.257(3) Å	□= 90°.
	b = 18.825(4) Å	□= 106.316(2)°.
	c = 14.403(3) Å	□ = 90°.
Volume	3189.5(12) Å^3	
Z	4	

Density (calculated)	1.282 Mg/m^3
Absorption coefficient	0.599 mm^{-1}
F(000)	1296
Crystal size	0.5 x 0.392 x 0.262 mm^3
Theta range for data collection	1.828 to 24.480°.
Index ranges	-14<=h<=14, -21<=k<=21, -16<=l<=16
Reflections collected	28726
Independent reflections	5256 [R(int) = 0.0429]
Completeness to theta = 24.480°	99.4 %
Absorption correction	Semi-empirical from equivalents
Max. and min. transmission	0.7450 and 0.6635
Refinement method	Full-matrix least-squares on F^2
Data / restraints / parameters	5256 / 0 / 375
Goodness-of-fit on F^2	1.022
Final R indices [I>2sigma(I)]	R1 = 0.0416, wR2 = 0.0911
R indices (all data)	R1 = 0.0643, wR2 = 0.1064
Extinction coefficient	n/a
Largest diff. peak and hole	0.341 and -0.226 $e.Å^{-3}$

Figure S24. Molecular structure of **Fe*-2.**

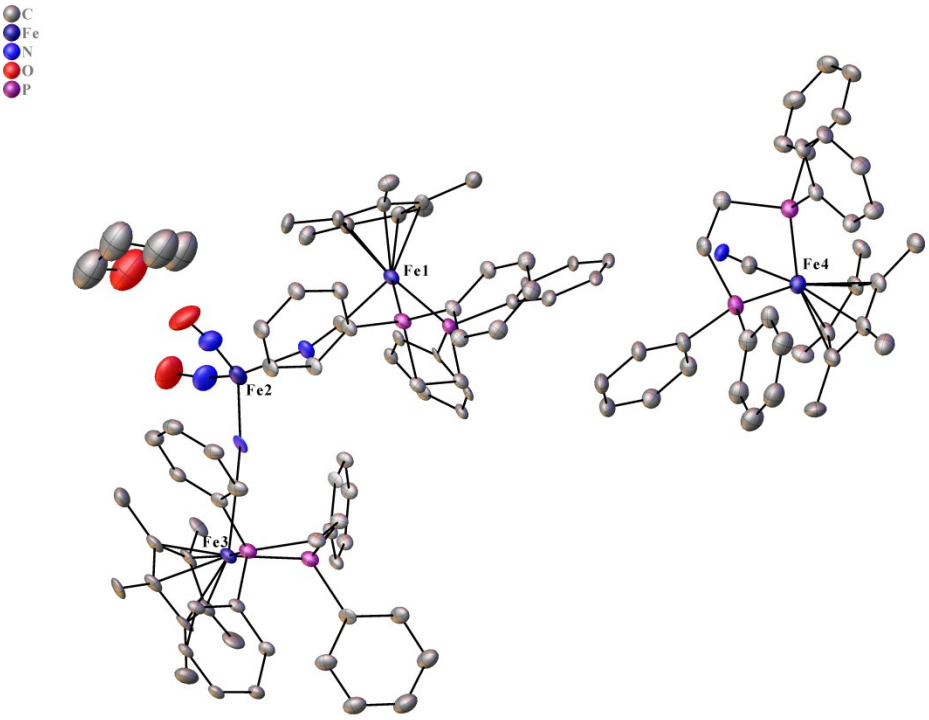

Table T4. Crystal data and structure refinement for **Fe*-2.**

Identification code	mqb	
Empirical formula	C114.40 H123.80 Fe4 N5 O2.85 P6	
Formula weight	2023.60	
Temperature	100.0 K	
Wavelength	1.54178 Å	
Crystal system	Triclinic	
Space group	P-1	
Unit cell dimensions	a = 18.1733(14) Å	□= 103.179(2)°.
	b = 18.5346(14) Å	□= 113.672(2)°.
	c = 20.2827(15) Å	□ = 106.712(2)°.
Volume	5514.3(7) Å^3	
Z	2	

Density (calculated)	1.219 Mg/m^3
Absorption coefficient	5.345 mm^{-1}
F(000)	2124
Crystal size	0.178 x 0.043 x 0.01 mm^3
Theta range for data collection	2.58 to 40.10°.
Index ranges	-15<=h<=15, -15<=k<=15, -16<=l<=16
Reflections collected	33016
Independent reflections	6720 [R(int) = 0.1083]
Completeness to theta = 40.097°	99.5 %
Absorption correction	Semi-empirical from equivalents
Max. and min. transmission	0.7479 and 0.6215
Refinement method	Full-matrix least-squares on F^2
Data / restraints / parameters	6720 / 2133 / 1207
Goodness-of-fit on F^2	1.057
Final R indices [I>2sigma(I)]	R1 = 0.0702, wR2 = 0.1184
R indices (all data)	R1 = 0.1074, wR2 = 0.1323
Extinction coefficient	n/a
Largest diff. peak and hole	0.567 and -0.497 $e.Å^{-3}$

Figure S25. Molecular structure of **$(Me_3P)_2Fe(NO)_2$.**

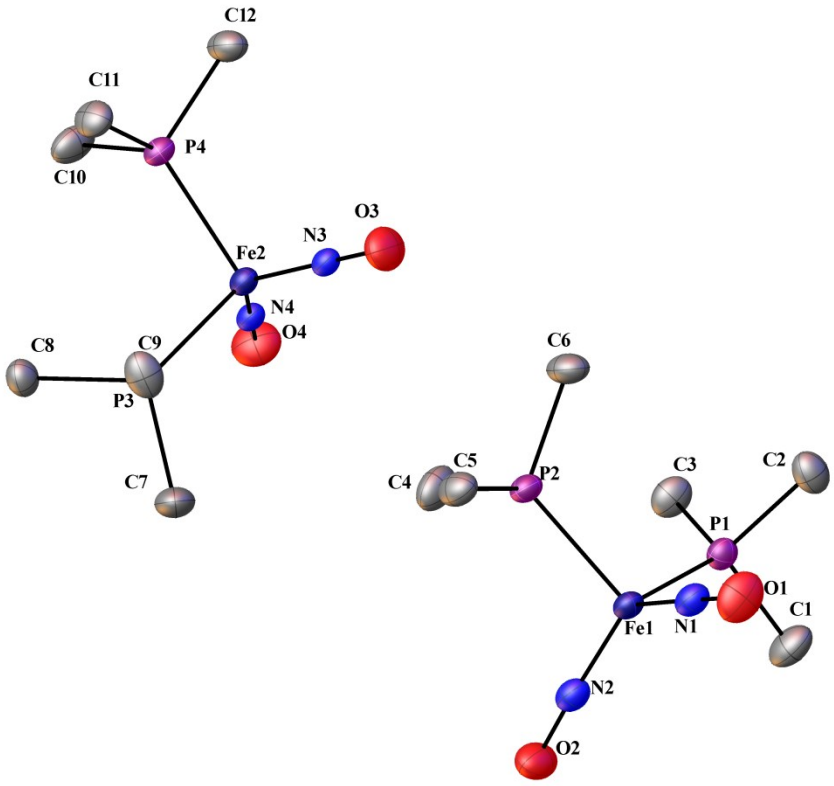

Table T5. Crystal data and structure refinement for **$(Me_3P)_2Fe(NO)_2$.**

Identification code	4	
Empirical formula	C6 H18 Fe N2 O2 P2	
Formula weight	268.01	
Temperature	150.15 K	
Wavelength	0.71073 Å	
Crystal system	Triclinic	
Space group	P-1	
Unit cell dimensions	a = 7.314(2) Å	α= 119.081(3)°.
	b = 13.917(4) Å	β= 90.263(3)°.
	c = 14.263(4) Å	γ = 93.646(4)°.
Volume	1265.2(7) $Å^3$	

Z	4
Density (calculated)	1.407 Mg/m^3
Absorption coefficient	1.421 mm^{-1}
F(000)	560
Crystal size	0.3 x 0.27 x 0.2 mm^3
Theta range for data collection	1.635 to 24.993°.
Index ranges	-8<=h<=8, -16<=k<=14, 0<=l<=16
Reflections collected	4408
Independent reflections	4408 [R(int) = 0.0441]
Completeness to theta = 24.993°	99.0 %
Absorption correction	Semi-empirical from equivalents
Max. and min. transmission	0.746 and 0.509
Refinement method	Full-matrix least-squares on F^2
Data / restraints / parameters	4408 / 0 / 229
Goodness-of-fit on F^2	0.999
Final R indices [I>2sigma(I)]	R1 = 0.0379, wR2 = 0.1002
R indices (all data)	R1 = 0.0513, wR2 = 0.1058
Extinction coefficient	n/a
Largest diff. peak and hole	0.592 and -1.032 $e.Å^{-3}$